

**TRACE and ground-based observations of microflares<sup>(\*)</sup>**G. CAUZZI<sup>(1)</sup>, A. FALCHI<sup>(1)</sup>, R. FALCIANI<sup>(2)</sup>, L. A. SMALDONE<sup>(3)</sup> and R. SHINE<sup>(4)</sup><sup>(1)</sup> *Osservatorio Astrofisico di Arcetri - Largo E. Fermi 5, 50125 Firenze, Italy*<sup>(2)</sup> *Dipartimento di Astronomia e Scienza dello Spazio, Università di Firenze  
Largo E. Fermi 5, 50125 Firenze, Italy*<sup>(3)</sup> *Dipartimento di Scienze Fisiche, Università di Napoli "Federico II"  
via Cintia, 80126 Napoli, Italy*<sup>(4)</sup> *Lockheed Martin Advanced Technology Center - 3251 Hanover Street, Palo Alto  
CA 94304, USA*

(ricevuto il 10 Giugno 2002; approvato il 7 Agosto 2002)

**Summary.** — We present high temporal and spatial resolution, multiwavelength observations of small-scale activity phenomena. The data were obtained during a coordinated campaign between ground-based and space observatories. Our analysis supports the concept that small flares are just *miniature* flares, *i.e.* that the same physical processes are at work, but that it is mandatory to have an excellent resolution in order to clearly identify them. In particular, we find that chromospheric downward motions are a very distinctive characteristic of the flare phenomenon even in tiny events.

PACS 96.60.-j – Solar physics.

PACS 96.60.Na – Chromosphere and chromosphere-corona transition; spicules.

PACS 96.60.Rd – Flares, bursts, and related phenomena.

PACS 01.30.Cc – Conference proceedings.

**1. – Introduction**

Small-scale activity phenomena (*e.g.*, microflares, nanoflares) have received unprecedented attention in the last few years, following the high-resolution observations provided by satellites such as SOHO and TRACE. Why are they so important? First of all, being virtually ubiquitous on the solar surface, small-scale transient phenomena could provide at least part of the coronal heating input. Second, if small flares are governed by the same physical mechanisms as the large ones, they could more clearly display the basic processes at work.

---

(\*) Paper presented at the International Meeting on THEMIS and the New Frontiers of Solar Atmosphere Dynamics, Rome, Italy, March 19-21, 2001.

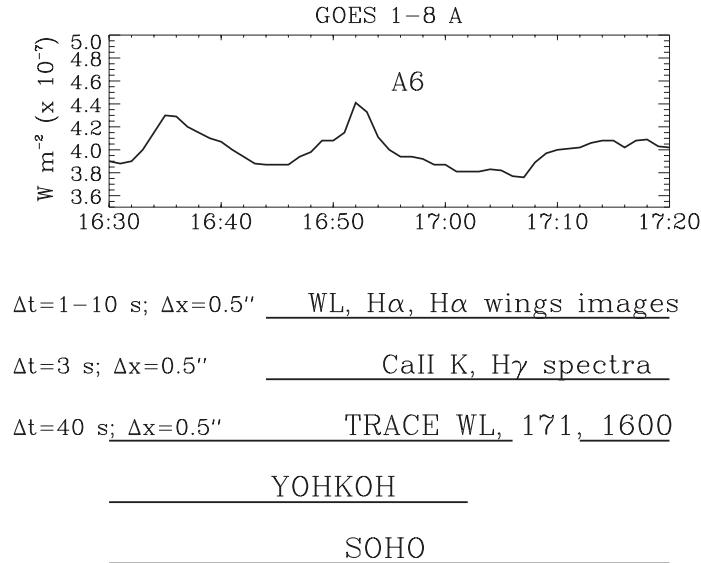


Fig. 1. – Top: the GOES 1–8 Å curve for the event described in text. The soft–X-ray class is A6, usually associated with “microflares”. Bottom: scheme of the coordinated observations obtained around the time of the microflare.

Up to now, most of the work on nano and microflares has been done using coronal signatures (see, among many others, [1-3]). However, as pointed out in the review by Falchi in these proceedings [4], the chromospheric dynamics in flares can be an important probe of the flare energetics and of the mechanisms for energy transport from the corona to the lower atmosphere. We hence present in the following a search for chromospheric signatures of small-scale activity phenomena, in particular of impulsive downward motions that could betray the “impact” site of a flaring event.

To this end, we obtained high spatial AND temporal resolution observations in several wavelengths, from coordinated observations involving both ground and space instruments. Such a data set is necessary in order to unambiguously identify a flaring event, and to study its associated manifestation at small scales.

## 2. – Observations

A GOES event of class A6 was observed at about 16:52 UT on Feb. 9, 1999, within the active region NOAA 8456. Such soft–X-ray class is usually associated with *microflares*, *i.e.* flares releasing  $10^{27-28}$  ergs [5]. The GOES 1–8 Å soft–X-ray curve of the event is shown in fig. 1, together with a very schematic summary of the data acquired.

The ground-based data were acquired with the cluster of instruments at the DST of NSO/Sac Peak. The field of view (FOV) of the ground-based images was about  $2 \times 2$  arcmin, with a pixel size of  $0.5''$ . White-light images were acquired as context images, and to provide a reference for the overlapping with space-based data (see below).  $H\alpha$  line center, and  $H\alpha$  wings ( $\pm 1.5$  Å) images were acquired for their importance in defining the various phases of the flare phenomenon [4]. The temporal resolution was quite high, ranging from 1 to 10 s depending on the wavelength.

The main diagnostic tool is given by the spectra acquired in the lines Ca II K and

$H\gamma$ , necessary for measuring the chromospheric downward motions associated with the impulsive phase of a flare [6]. During the observations, the slit was left in a fixed position within the FOV, and spectra were continuously acquired every 3 s, providing a very high cadence suited to the highly dynamical nature of (small) flares.

TRACE images at full resolution ( $0.5''$  /pixel) were acquired on a FOV of about  $6 \times 6$  arcmin in three wavelengths: 171 Å, 1600 Å, and white light, with a cadence of 40 s. The 171 Å band contains emission lines of Fe IX/X, and is representative of plasma at temperatures around 1 MK [7], *i.e.* of the transition region or low corona. The broadband 1600 Å images provide diagnostics of the UV continuum, and sample temperatures ranging from 4000 to 10000 K.

Finally, the data acquired by Yohkoh (mainly SXT) and SOHO (EIT) complete the height coverage in the atmosphere providing a sampling at coronal temperatures. In the following, we will limit the analysis to ground-based and TRACE data.

The seeing conditions on the ground were fairly good during the observing period of about 1 h, so the effective spatial resolution was close to that of TRACE,  $1''$ . The white-light data acquired both from the ground and with TRACE allowed an excellent overlapping of the two sets of images, with a precision estimated at about  $1''$  throughout the whole period of common observations.

### 3. – Temporal analysis

Figure 2a shows a small portion of the FOV in  $H\alpha + 1.5$  Å, at the time of the GOES maximum (16:52 UT). Although visible in the disk-integrated soft–X-ray emission, the flare kernel is really small, just a few arcsec across. As is the case for much bigger flares, the red wing of  $H\alpha$  shows structures much more compact, and with a more impulsive behavior, than the ones visible in the center of  $H\alpha$  (not shown in figure). As reviewed by Falchi [4], this often leads to the assumption that the emission in the  $H\alpha$  red wing can be used as a proxy for chromospheric velocity, *i.e.* that it maps the “impact” site of an accelerated electron beam, or of a conduction front, onto the lower atmosphere. We will return on this subject later in the paragraph.

Figure 2b is a simultaneous, co-spatial 171 Å image from TRACE. The dimensions and, to a smaller extent, the shape of the bright kernels appear rather similar in both  $H\alpha$  red wing and 171 Å images throughout the flare evolution. This might indicate that the EUV emission maps only the lower portion of the flaring coronal loops, *i.e.* more or less the same “footpoints” observed at lower layers.

Figures 2c and d display stacks of Ca II K spectra acquired in two different positions along the slit, as indicated by the arrows. The spectra are displayed on the same intensity scale. The main flaring episode is readily visible in panel d as an increased emission starting slightly before 16:52 UT, and is clearly characterized by strikes in the red wing of the line. Such red asymmetries in chromospheric lines are observed in the impulsive phase of bigger flares, and explained in terms of downward motions induced on the chromospheric layer by the impact of an electron beam, or of a conduction front (see, for example, [8] and [9], respectively). Given the impulsiveness of the motions, and the compactness of the regions involved, one can assume that the downward motions clearly map the footpoints of the flaring loops. The asymmetries displayed in fig. 2d are indeed limited to a narrow ( $2$ – $3''$ ) region along the slit, precisely pin-pointing the site of energy deposition in the chromosphere for this small event. The velocities deduced from the line asymmetries are of the order of 10 km/s (see also fig. 3), *i.e.* well comparable with those measured in major flares, that average around 50 km/s [6].

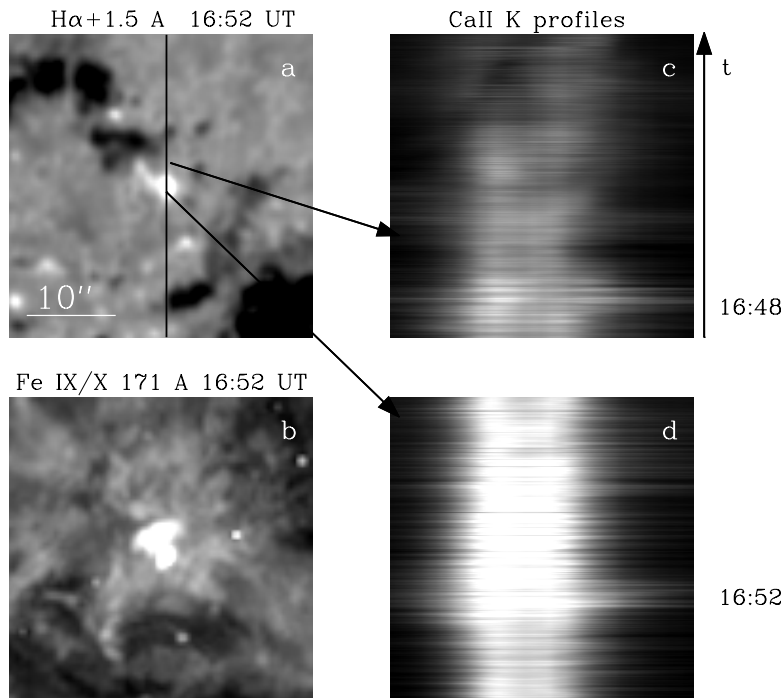


Fig. 2. – a)  $H\alpha +1.5 \text{ \AA}$  image of a portion of the FOV, acquired at the time of maximum GOES emission. The black line represents the spectrograph slit within the FOV. b) Same as a), for the TRACE 171  $\text{\AA}$  wavelength. c), d) Temporal series of Ca II K spectra acquired in the two positions indicated by the arrows. The lower one corresponds to the main flaring location. The  $x$ -axis translates into Doppler velocities of  $-40 \text{ km/s}$  (upward) and  $+50 \text{ km/s}$  (downward).

Figure 2c shows the spectra acquired in a region slightly above the main flare kernel. The emission is always much less intense than in the former case, but also in this portion of the slit an enhancement accompanied by impulsive emission in the red wing is clearly visible, occurring a few minutes prior to the main flaring event. Corresponding velocities reach the value of  $20 \text{ km/s}$  over an area less than  $2''$  wide. This same area also shows simultaneous small and fluctuating brightenings at all other wavelengths, *i.e.* it displays a behavior typical of the so-called “precursor” phenomenon often observed in major flares. It seems safe to conclude that, at least in this case, the precursor activity is due to another flare, just more limited in the total duration and emission and probably falling below the detecting threshold for signatures such as X-rays.

In fig. 3 we plot the chromospheric velocity, as deduced from the Ca II K analysis, *vs.* the light curves of Fe IX/X 171  $\text{\AA}$  (left column) and  $H\alpha$  red wing (right column), for the duration of the observations. The  $H\gamma$  spectra provide essentially the same information. The two rows refer to the upper and lower (main) flare kernels described above. The curves of fig. 3 are obtained averaging over an area of about  $3 \times 3 \text{ arcsec}$  ( $3 \text{ arcsec}$  along the slit for the velocity). Some contamination from one kernel to another is present since the two features are so close together.

The curves of chromospheric velocities for both kernels display an impulsive behavior that clearly indicate the time of impact of the coronal disturbance. The amplitude of the

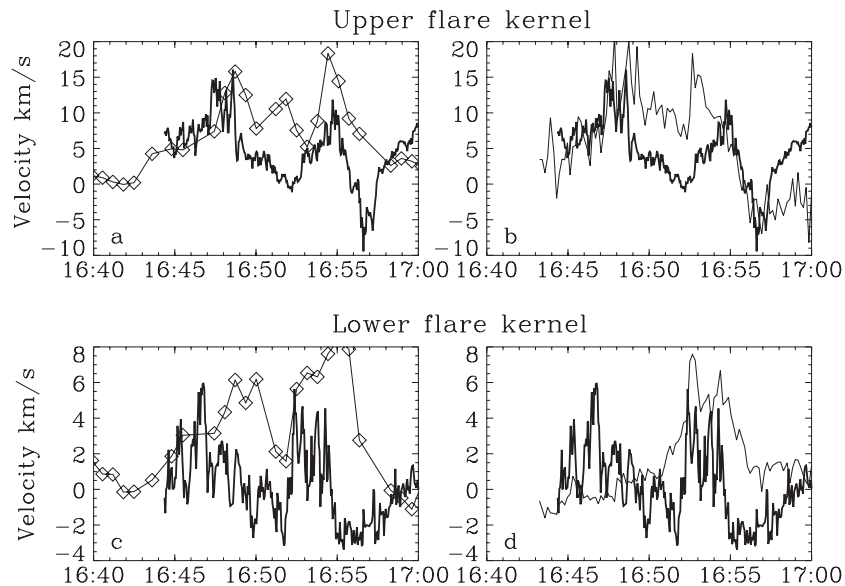


Fig. 3. – a) Chromospheric velocities in the upper flaring kernel (thick line), *vs.* light curve of Fe IX/X 171 Å (thin line). b) Same as a), but thin line now represents the H $\alpha$  + 1.5 Å curve. Curves for Fe IX/X and H $\alpha$  + 1.5 Å are displayed on arbitrary scales. c), d) Same as a), b), for lower (main) flaring kernel.

motion is sensibly higher for the upper kernel, contrary to what one might expect from the relative importance of the two events. Most probably, pre-existing conditions such as an already perturbed, denser atmosphere have a role in determining the net effect of the energy deposition onto the chromosphere (see discussion in [4]).

The Fe IX/X curves reach their maximum few minutes after the appearance of the chromospheric downflows. This might be explained if the chromosphere undergoes an explosive evaporation filling the flaring loop with plasma heated at coronal temperatures, that later cools off to the  $\approx 1$  MK temperature giving rise to EUV emission.

Finally, a comment on the H $\alpha$  + 1.5 Å curves: for the upper flare kernel (fig. 3b), the H $\alpha$  + 1.5 Å curve closely resembles the chromospheric velocity curve, showing an impulsive enhancement within few seconds of the impulsive downward motion developing at 16:48 UT. In this case, the use of this spectral signature as a proxy for the chromospheric velocity seems largely justified. However, such a tight correlation does not hold for the main flaring episode of 16:52 (fig. 3d): in this case, the H $\alpha$  red wing curve shows a much broader rise, with a less impulsive behavior than the velocity. This fact might be due an atmosphere already modified by the (nearby) previous energy deposition, or simply show that the H $\alpha$  line is sensitive to different aspects of the flare phenomenon, and cannot always be substituted to velocity measurements.

#### 4. – Conclusions

We have obtained high spatial and temporal resolution multiwavelength data covering the development of a microflare. The coordinated observations allow us to get a good coverage of the flare throughout the atmosphere, and to clearly identify the different

aspects of the phenomenon.

All of our data support the idea that microflares are just *miniature* flares. From our first analysis, we can state that all the relevant signatures normally detected in a major flare are visible also in this small event, with the same sequentiality. A more complete analysis will take into account also EIT and, especially, Yohkoh/SXT data, in order to better substantiate this picture.

Of particular relevance is the finding that at chromospheric levels one observes downward motions in the (presumed) footpoints of the flaring loops also for small events, and that these motions have amplitudes well comparable with those measured for major flares. To us, this clearly shows that the same physics is at work, provided that one has sufficient resolution to observe it! The same kind of motions are visible in other small events occurred during the observations, for which a more thorough analysis of the data is underway.

Finally, a decisive improvement in the study of micro and nanoflares will come from the HESSI satellite [10] that will be able to provide imaging at hard-X-ray wavelengths with spatial resolution as high as  $2''$ . It will be most interesting, for example, to compare the site of production of hard-X-ray with the location of the chromospheric downflows.

#### REFERENCES

- [1] KRUCKER S. and BENZ A. O., *Astrophys. J.*, **501** (1998) L213.
- [2] BERGHMANS D., CLETTE F. and MOSES D., *Astron. Astrophys.*, **336** (1998) 1039.
- [3] ASCHWANDEN M. J., NIGHTINGALE R. W., TARBELL T. D. and WOLFSON C. J., *Astrophys. J.*, **535** (2000) 1027.
- [4] FALCHI A., this issue, p. 639.
- [5] FELDMAN U., DOSCHECK G. A. and BEHRING W. E., *Astrophys. J.*, **461** (1996) 465.
- [6] ICHIMOTO K. and KUROKAWA K., *Solar Phys.*, **93** (1984) 105.
- [7] HANDY B. N. *et al.*, *Solar Phys.*, **187** (1999) 229.
- [8] FISHER G. H., CANFIELD R. C. and MCCLYMONT A. N., *Astrophys. J.*, **289** (1985) 414.
- [9] GAN W. Q., FANG C. and ZHANG H. Q., *Astron. Astrophys.*, **241** (1991) 618.
- [10] SCHMAHL E. J., *Imaging Hard X-ray Flares with HESSI*, in *AGU Spring Meeting 2001*, abstract #SP51A-10.